



# Novel medium-and long-chain triacylglycerols rich structured lipids enriched in n-3 polysaturated fatty acids encapsulated by spray drying: Characterization and stability

Imad Khan<sup>1</sup>, Mudassar Hussain<sup>1</sup>, Adil Khan<sup>2</sup>, Bangzhi Jiang<sup>1</sup>, Lei Zheng<sup>1</sup>, Shamim Hossain<sup>1</sup>, Waleed AL-Ansi<sup>1</sup>, Xiaoqiang Zou<sup>1\*</sup>

<sup>1</sup>State Key Laboratory of Food Science and Resources, National Engineering Research Center for Functional Food, National Engineering Research Center of Cereal Fermentation and Food Biomanufacturing, Collaborative Innovation Center of Food Safety and Quality Control in Jiangsu Province, School of Food Science and Technology, Jiangnan University, 1800 Lihu Road, Wuxi 214122, Jiangsu, China

<sup>2</sup>Key Laboratory of Industrial Biotechnology, Ministry of Education, Jiangnan University, Wuxi 214122, China.

\* Corresponding author: Xiaoqiang Zou, email: xiaoqiangzou@163.com

Received: 01 Feb 2024; Received in revised form: 15 Mar 2024; Accepted: 25 Mar 2024; Available online: 03 Apr 2024

©2024 The Author(s). Published by Infogain Publication. This is an open access article under the CC BY license

<https://creativecommons.org/licenses/by/4.0/>.

**Abstract**— Novel MLCTs-rich SLs, enriched with n-3 PUFAs, were synthesized to combine the benefits of docosahexaenoic acid (DHA), eicosapentaenoic acid (EPA), and medium-chain FAs (MCFAs). However, these SLs were susceptible to oxidative degradation. To solve this issue, the MLCT-rich SLs were microencapsulated using different wall materials through spray drying technique. Initially, in this study three formulations of different wall materials were designed: modified starch/maltodextrin [MS/MD (2:1)], gum Arabic/maltodextrin [GA/MD (2:1)], and mixed [MIX (MS:GA:MD, 1:1:1)]. Subsequently, all the three formulations were analysed. The analysis included encapsulation yield, encapsulation efficiency, moisture content, hygroscopicity, water activity, density properties, Carr's index, cohesiveness, flowability, porosity, wettability, solubility, color, and relative crystallinity. Fourier transform infrared spectroscopy (FTIR) was employed to identify the chemical structure of the microcapsule powder. The moisture content ranged from 1.71% to 3.45%, while water activity ranged from 0.17 to 0.31 of all formulations, indicating suitability for long-term storage. Additionally, the highest microencapsulation yield (93.23%) and microencapsulation efficiency (93.74%) were achieved with GA/MD formulation. GA/MD also exhibited the highest relative crystallinity (32.50%). Moreover, FTIR analysis confirmed the successful encapsulation of the oil in the microcapsules. Furthermore, scanning electron microscopy (SEM) images revealed spherical shapes without any visible cracking on the surfaces of the microcapsules. Besides, GA/MD formulation demonstrated better results in density properties, flowability, porosity, and wettability. During the oxidative stability, GA/MD microencapsulation provided the best protection against lipid oxidation. These findings highlight the effectiveness of using GA/MD formulation for the production of microcapsule powders containing MLCTs-rich SLs.



**Keywords**— Medium and Long-Chain Triacylglycerols; n-3 Polyunsaturated Fatty Acids; Bio-imprinted Lipase; Interesterification; Microencapsulation

## I. INTRODUCTION

Structured lipids (SLs) can be produced enzymatically or chemically via interesterification, acidolysis, and/or

esterification processes from the conventional fats/oils in order to improve their nutritional and functional properties (Lu et al., 2017). SLs are available in a number of

commercial zero- or low- calorie food ingredients, for example salatrim (Nabisco, USA) and diacylglycerol (Kao Cooperation, Japan). Medium and long-chain triacylglycerols (MLCTs) are a special kind of SLs found in food products like Resetta™ (Nisshin Oillio Group Ltd., Japan) that have been found with many physiological benefits, such as anti-obesity effect and the maintenance of good cholesterol (Lee et al., 2015). Furthermore, MLCTs possess the capability to provide the body with quick energy and essential fatty acids such as arachidonic acid (ARA) by an easy way, thus they are very useful for humans, in particular for infants (Korma et al., 2018). Polyunsaturated fatty acids (PUFAs) are FAs with more than one double bond. Omega-3 (n-3) PUFAs include eicosapentaenoic acid (EPA), docosahexaenoic acid (DHA) and alpha-linolenic acid (ALA). The health benefits related to n-3 PUFAs are reported in several studies (Calder, 2020; Khan et al., 2023). The consumption of EPA and DHA helps in the treatment and prevention of inflammatory, neurological, and cardiovascular diseases (Jiang et al., 2022; Khan et al., 2023). Fish oil is abundant in EPA and DHA but contains very low concentration of ALA. Examples of fish oils with the highest concentrations of EPA and DHA include tuna, anchovy, sardine, cod, and salmon, among others. Nevertheless, the reported concentration of DHA in different fish oils ranges from 10% to 30%. The derivation of DHA and EPA from fish oils has been demonstrated through both chemical and enzymatic processes (Ackman & Burgher, 1963). Therefore, it is important to reduce the oxidation of ARA, in order to improve their quality in food applications.

In the encapsulation method, the wall materials have an excellent influence on the physical and functional properties of the microencapsulated products (Premi & Sharma, 2017). Maltodextrin (MD), gum arabic (GA), and whey protein isolate (WPI) are the most frequently applied wall materials for microencapsulation of oils (Chew et al., 2018; Korma et al., 2019). Maltodextrin is the most commonly used wall material due to its low cost, low viscosity at a high solid concentration, neutral taste, and well protection against oxidation with low capacity for emulsifying (de Barros Fernandes et al., 2014). Thus, the MD preferred only in various combinations with other carrier agents such as WPI and GA. GA exhibits low viscosity, high solubility, and good emulsifying characteristics that make it an appropriate wall material (Korma et al., 2019). The utilization of WPI as an encapsulating agent in the food industry is very appealing due its extensive nutritional benefit. Besides, the presence of hydrophilic and hydrophobic amino acids of whey protein smoothens the encapsulation of compounds of the hydrophobic nature (Premi & Sharma, 2017). In recent decades, researchers applied microencapsulation with

different carriers and techniques to improve the quality and stability of oils (Bakry et al., 2016). Consequently, the stability, nutritional quality, and health properties of several vegetables, marine, and seed oils have been improved by microencapsulation (Bakry et al., 2016).

In order to improve the applicability of MLCTs-rich SLs rich in n-3 PUFAs as lipid ingredient in nutritional and functional food applications, MLCTs-rich SLs could be transformed into powder and encapsulated on food products by spray drying technology. Hence, the aims of this study were to investigate the development of a combination of the gum arabic, maltodextrin, and modified starch, as wall materials for microencapsulation of the MLCTs-rich SLs by spray drying, and to evaluate the physicochemical characteristics and oxidative stability of the encapsulated MLCTs-rich SLs during storage.

## II. MATERIALS AND METHODS

### 2.1. Materials

MS was purchased from Hilmar ingredients (Tianjin Milky way import & export Co., Ltd., China). GA was procured from Sinopharm (Chemical Reagent Co., Ltd., China). MD was provided by Shyuanye Co. China. OMAX 1812 fish oil (a mixture of anchovy and sardine oils) was purchased from NovoSana Co., Ltd (China). MCTs containing 60% caprylic acid and 40% capric acid were obtained from J&K Scientific Ltd. Under controlled conditions in sealed bags. In all experiments, the high purity and analytical grade chemicals were used.

### 2.2. Production and purification of MLCTs-rich SLs

The best conditions achieved the highest yield of MLCTs-rich SLs were selected for the scale production of MLCTs-rich SLs according to our previous study. The solvent-free interesterification reaction was performed in a 500 mL stirred batch reactor at 70 °C for 3 h with a substrate's mole ratio of ARASCO: MCTs (1:1.5 mol/mol), 4% (w/w) of bio-imprinted NS 40086 lipase, and constant stirring at 600 rpm. The reactor was covered with foil to decrease exposure to light. At the end of the reaction, the resulting of MLCTs-rich SLs was collected after removal of the enzyme by filtration. Purification of MLCTs-rich SLs product was performed according to the method described by (Korma et al., 2018). The free fatty acids of MLCTs-rich SLs were reduced from 2.7 to 0.13 %, and determined by the method reported by Firestone (2009). Purified MLCTs-rich SLs were stored in an airtight amber container under nitrogen at -20 °C. The major fatty acids in the synthesized SLs were EPA, DHA, caprylic, and capric acids.

### 2.3. MLCTs rich SLs emulsion preparation

Three formulations were used based on the method outlined by Chew et al. [275], with some modifications. These formulations consisted of (GA/MD, 2:1), (MS/MD, 2:1), and mixed (MIX) (GA/MS/MD, 1:1:1) wall materials (Table 1). Firstly, the wall materials were dissolved in distilled water on the day before emulsification and kept overnight at room temperature to ensure the full hydration of the polymer molecules of the materials. Then the MLCTs-rich SLs were then dispersed in these solutions

using a high-speed homogenizer (Ultra-Turrax IKA T18 basic, Wilmington, NC, USA) at 22,000 rpm for 4 min at room temperature. A fine emulsion was then formed by passing the dispersion through an ATS AH2100 high pressure homogenizer (AH- 2010, ATS Engineering Inc., Canada) operated at 40 MPa with 4 processing cycles. The resulting emulsions were stored at 4 °C with 0.02% (w/v) sodium azide as an antimicrobial agent until further analysis.

Table 1. Description of formulation.

Treatments	Wall materials (g/100g)			Core materials (g/100g) MLTs rich SLs	Wall to the core ratio	Total solid to the water ratio
	MD	MS	GA			
MS/MD	33.33 g	66.67 g	-	33.33 g	3:1	30:70
GA/MD	33.33 g	-	66.67 g	33.33 g	3:1	30:70
MIX	33.33 g	33.33 g	33.33 g	33.33 g	3:1	30:70

Abbreviations: MS = modified starch; MD = maltodextrin; GA = gum Arabic; MIX = mixed

#### 2.4. Microencapsulation by spray drying

The microcapsules containing MLCTs-rich SLs were produced by drying the homogenized MLCTs-rich SLs emulsions using a GEA Niro spray dryer (model Mobile Minor™, Soborg, Denmark). The emulsions were added into the drying chamber through a peristaltic pump at a feed flow rate of 14 - 15 mL min<sup>-1</sup>. Operating parameters for the spray dryer included inlet and outlet temperatures set at 180 °C ± 5 °C and 80 °C ± 5 °C, respectively, with an airflow rate of 300 NL min<sup>-1</sup>. The resulting dried powder was then collected and stored in sealed plastic bags at -20 °C for further analysis.

#### 2.5. Characterization of spray dried microcapsules

##### 2.5.1. Microencapsulation yield

The encapsulation yield post-spray drying was determined as a percentage, calculated by dividing the total weight of the microcapsule powders by the weight of the carrier agents, according to Equation (1).

$$\text{Encapsulation yield (\%)} = \frac{\text{weight (g) of the collected powder}}{\text{weight (g) of the carrier agents}} \times 100 \quad (1)$$

##### 2.5.2. Microencapsulation efficiency of total oil (TO), and surface oil (SO)

The TO content within the particles was determined through cold extraction with an organic solvent. Initially, 8 millilitres of distilled water were added to 2.5 grams of powder in a glass tube equipped with a screw cap, which was then placed in an ultrasound bath for 5 minutes at room temperature. Following this, 10 mL of chloroform and 20

mL of methanol were added into the tubes, following the methodology outlined by (Bligh & Dyer, 1959). The tubes were sealed with tape and the lids, and manually shaken by inversion of 50 times. After adding an additional 10 mL of chloroform, the tubes were shaken for an additional 2 minutes and then left undisturbed for 30 minutes to allow for phase separation. The upper hydrophilic phase (containing methanol and water) was discarded. The remaining sample in the lower chloroform phase was filtered through a Whatman filter paper no. 1. A 5 mL aliquot of the filtered solution was transferred to an oven at 100°C for 1 hour to completely evaporate the solvent. The remaining mass in the beaker was considered as the total oil content present in the particles.

The SO was evaluated following a method described by (Bae & Lee, 2008), with certain modifications. Initially, 1.5 grams of powder were washed with 15 millilitres of hexane in a glass tube with a screw cap for 2 minutes at room temperature. The resulting mixture was then filtered through a Whatman filter paper no. 1. The powder collected on the filter was rinsed three times with 20 mL of hexane. Subsequently, the solvent was allowed to evaporate at 60°C until a constant weight was achieved. The non-encapsulated oil was determined by the difference in mass between the initial clean flask and the one containing the extracted oil residue, following methods outlined by (Carneiro et al., 2013).

Both TO and SO determinations were used to calculate the microencapsulation efficiency (M. E. E) using Equation (2) as described by (Bae & Lee, 2008).

$$\text{M.E. E} = \left( \frac{\text{TO-SO}}{\text{TO}} \right) \times 100 \quad (2)$$

### 2.5.3. Moisture content

The moisture content of the microcapsule powders was assessed using the air oven method, as detailed in reference (Kang et al., 2019). The moisture content was determined by measuring the weight loss after drying the sample in a drying oven at 105°C until a constant weight was achieved. This process is represented by Equation (3):

$$\text{Moisture content (\%)} = \frac{\text{wet sample weight (g)} - \text{dry sample weight (g)}}{\text{wet sample weight (g)}} \times 100 \quad (3)$$

### 2.5.4. Water activity (aw)

The water activity of the microcapsule powders was determined using an electronic water activity meter (Labmaster-aw, Novasina AG, Neuheimstrasse, Switzerland) following stabilization of the microcapsule powder samples at 25°C for 15 minutes, as described by (Santhalakshmy et al., 2015).

### 2.5.5. Hygroscopicity

The hygroscopicity of the microencapsulates was evaluated following the method outlined by Cai and Corke (Cai & Corke, 2000), with minor modifications. Initially, approximately 0.5 grams of each sample were placed in a preweighed petri dish. These dishes were then placed in a desiccator filled with a saturated NaCl solution (75% relative humidity) at 25°C. After one week, the samples were removed from the desiccator and reweighed. The hygroscopicity of the samples was determined based on the change in weight observed over the test period.

### 2.5.6. Wettability

The wettability of each sample was evaluated by determining the time (minutes) needed to immerse 1 gram of microcapsule powder on the surface of 400 mL of distilled water at a temperature of 25°C (Mahdi et al., 2020).

### 2.5.7. Solubility

The solubility of the microcapsule powders was evaluated following the method outlined by (Santhalakshmy et al., 2015). Specifically, 1 gram of microcapsule powder was mixed and transferred into 100 mL of distilled water. The mixture was then stirred using a magnetic stirrer at 500 rpm for 30 minutes at 25°C, followed by centrifugation at 3000 rpm for 5 minutes. An aliquot of 25 mL of the supernatant was dried at 105 °C. Solubility of the microcapsule's powders were then calculated using equation (4):

$$\text{Solubility (\%)} = \frac{\text{weight of the powder (g) in the supernatant}}{\text{weight of the powder (g) in the solution}} \times 100 \quad (4)$$

### 2.5.8. Bulk density (BD)

The BD of the sample powders was analysed following the procedure outlined by (Saifullah et al., 2016). In summary, 2.0 grams of the powder sample were added into a 10 mL graduated measuring glass cylinder. The bulk density was subsequently calculated using equation (5):

$$\text{BD (g/cm}^3\text{)} = \frac{\text{sample weight (g)}}{\text{sample volume (cm}^3\text{)}} \quad (5)$$

### 2.5.9. Tapped density (TD)

The TD was evaluated following the procedure described by (Saifullah et al., 2016). To measure the tapped volume of the samples, 2 grams of the powder were placed in a 10 mL graduated measuring glass cylinder. The cylinder was then tapped gently 100 times onto a rubber mat from a height of 20 cm. Subsequently, the tapped density was calculated using equation (6):

$$\text{TD (g/cm}^3\text{)} = \frac{\text{sample weight (g)}}{\text{sample volume (cm}^3\text{)}} \quad (6)$$

### 2.5.10. Particle density (PD)

PD was determined in accordance with the protocol outlined by (Santhalakshmy et al., 2015). In summary, 1.0 gram of powder was transferred into a 10 mL measuring cylinder equipped with a glass stopper. Approximately 5.0 mL of petroleum ether was then added, and the mixture was shaken for 30 seconds. Subsequently, the walls of the cylinder were rinsed with 2 mL of petroleum ether, and the total volume was recorded. The PD was calculated using equation (7):

$$\text{PD (g/cm}^3\text{)} = \frac{\text{sample weight (g)}}{\text{total volume of petroleum ether and suspended particles (cm}^3\text{)} - 7} \quad (7)$$

### 2.5.11. Flowability

The Flowability was estimated based on the Carr index (CI) and Hausner ratio (HR) (Saifullah et al., 2016). CI was used to express the flowability of the sample powders based on tapped and bulk densities (Saifullah et al., 2016). The CI of the microcapsules powders was calculated by using equation (8);

$$\text{carr index (\%)} = \frac{(\text{TD}-\text{BD})}{\text{TD}} \times 100 \quad (8)$$

Where TD is tapped density and BD is bulk density.

The cohesiveness of the samples was estimated using HR based on tapped and bulk densities (Saifullah et al., 2016). The HR was calculated using equation (9);

$$\text{hausner ratio} = \frac{\text{TD}}{\text{BD}} \quad (9)$$

where TD is tapped density and BD is bulk density.

### 2.5.12. Bulk porosity (BP)

The BP of the samples was determined according to the method reported by (Saifullah et al., 2016), based on PD and TD. BP was estimated using equation (10);

$$\text{bulk porosity (\%)} = \frac{(\text{PD}-\text{TD})}{\text{PD}} \times 100 \quad (10)$$

Where TD is tapped density and PD is particle density.

### 2.5.13. Color (L\*, a\*, and b\*) values

The color of the microcapsule powders was assessed using a colorimeter (HunterLab UltraScan PRO Spectrophotometer, Hunter Associates Laboratory, Inc., Virginia, USA). Before measurement, the instrument was calibrated to standard white and black tiles. About 5 g of microcapsule powder was placed in a transparent plastic bag, and the color parameters [L\* (light/dark), a\* (red/green), and b\* (yellow/blue)] were measured on three randomly selected surfaces of each sample (AL-Ansi et al., 2019).

### 2.5.14. Scanning electron microscope

The morphology of the microcapsules was examined using a scanning electron microscope (SEM), specifically the Hitachi High-Technologies Corp. SEM SU 1510 (Tokyo, Japan). Samples were fixed onto metal stubs using double-sided sticky tape, with dimensions of 1 cm in diameter and 1 cm in height. Prior to imaging, the samples were gold-coated using a sputter coater (Hitachi, E-1010) within a high-vacuum evaporator. Scanning was performed at an accelerating beam voltage of 3.0 kV and a magnification of 1000x.

### 2.5.15. Fourier transform infrared (FTIR)

The chemical structure was identified using the FT-IR spectrophotometer (Nicolet iS10, Thermo Fisher Scientific Co. Ltd., Waltham, Massachusetts, USA) according to the established method by (Hu et al., 2018). The sample powder was blended with KBr powder in a ceramic mortar and pressed into pellets. The FT-IR spectrum of the samples was measured at a resolution of 4 cm<sup>-1</sup> in transmission mode from 500 to 4000 cm<sup>-1</sup> wave length range.

### 2.5.16. Crystallinity (X-ray diffraction)

The crystallinity was evaluated using an X-ray diffractometer (D2PHASER, Bruker AXS Co. Ltd., Karlsruhe, Germany) (Li et al., 2018). The scanning region of the diffraction angle (2θ) ranged from 5° to 80°. X-ray diffraction patterns of samples were analysed using software (MDI Jade 6) and calculated as relative crystallinity (%) according to the following equation;

$$\text{RC (\%)} = \frac{\text{sum of total crystalline peak areas}}{\text{sum of the total crystalline and amorphous peak areas}} \times 100 \quad (11)$$

### 2.5.17. Oxidative stability under accelerated storage

The powder samples were subjected to accelerated storage conditions, maintained at 60°C for a duration of 28 days. At specific intervals of 0, 7, 14, 21, and 28 days, samples were collected from the storage and evaluated for peroxide value (PV) (Firestone, 1989).

### 2.6. Statistical evaluation

The experiments and sample measurements were replicated three times. Data analysis was performed using Microsoft Excel 2021 and Origin 9.9.0 software, and the results were presented as mean values accompanied by standard deviations. ANOVA (Analysis of Variance) was carried out using the Statistical Analysis System software (SAS, SPSS). A significance level of α = 0.05 was used, and any differences with a P-value < 0.05 were considered significant.

## III. RESULTS AND DISCUSSION

### 3.1. Encapsulation yield

The yields of microencapsulated MLCTs rich in SLs are presented in **Table 2**. During this study, the microencapsulation yield ranged from 85.34% to 93.23%, a range considered satisfactory based on the drying standard reported by Du et al. (Du et al., 2014). The results indicated that the GA/MD (93.23%) formulation exhibited the highest microencapsulation yield. Interestingly, there were no significant differences (p ≤ 0.05) observed between GA/MD and MIX formulations. This lack of difference may be attributed to the presence of GA in both formulations, as GA possesses a strong capability for film-forming. Conversely, the MS/MD (85.34%) formulation demonstrated the lowest microencapsulation yield, may be due to the absence of GA in its composition.

### 3.2. Microencapsulation efficiency

Microencapsulation efficiency (M.E.E) assists as a critical parameter for confirming the effectiveness of an encapsulation process, regardless of the methodology or core materials used (de Souza et al., 2018). It holds particular significance in evaluating the quality of oil encapsulation products, especially in the context of spray drying. The M.E.E values reported in this study were 90.34%, 93.74%, and 91.65% for MS/MD, GA/MD, and MIX microcapsules, respectively (**Table 2**). The spray-drying technique is preferred for producing powders with high M.E.E values, typically around 90% (Carneiro et al., 2013; Ng et al., 2013). In this study, all three formulations demonstrated excellent retention of MLCTs rich SLs, with M.E.E values exceeding 90%. GA/MD exhibited the highest M.E.E, followed by MIX. These outcomes suggest

that the polysaccharides utilized (GA and MD) enhanced M.E.E in this investigation. Similar findings were reported in other studies regarding microcapsules of refined kenaf (*Hibiscus cannabinus* L.) seed oil (Chew et al., 2018).

### 3.3. Moisture content and water activity

Moisture content and water activity are crucial indicators of powder quality and storage stability. The results revealed moisture contents of 3.45%, 1.71%, and 2.66% for microencapsulated MLCTs rich SLs in the MS/MD, GA/MD, and MIX treatments, respectively (**Table 2**). MS/MD exhibited a relatively higher moisture content (3.45%) compared to GA/MD (1.71%), attributed to the higher water-holding capacity of proteins in an amorphous state. Consequently, an increase in MS proportion resulted in higher moisture content in MS/MD. Conversely, in the GA/MD formulation, the incorporation of GA and MD in a 2:1 ratio led to a reduction in moisture content, enabling robust wall formation. Overall, all results indicated moisture contents below 4%, a desirable characteristic for powders, as the maximum moisture content for most powders used in the food industry is typically 4% (Karaca et al., 2013; Korma et al., 2019).

Water activity values for MS/MD, GA/MD, and MIX formulations are also presented in **Table 2**. Similar to the moisture content findings, the addition of GA and MD in a 2:1 ratio in the GA/MD formulation resulted in decreased water activity. Powders with water activity levels below 0.3 are deemed to possess high shelf-life stability against microbial growth (Drusch & Schwarz, 2006; Korma et al., 2019).

### 3.4. Hygroscopicity

Hygroscopicity refers to a material's ability to absorb moisture from the atmosphere, which can lead to fat oxidation in powders, affecting their nutritional value and flow. The hygroscopicity of MS/MD was significantly lower ( $p < 0.05$ ) compared to GA/MD and MIX formulations, with values of 6.75 g/100 g, 7.44 g/100 g, and 8.67 g/100 g, respectively (**Table 2**). It was previously suggested that samples with lower moisture contents would exhibit increased hygroscopicity, as the ability to absorb moisture is influenced by the water concentration gradient between the powder products and the atmosphere (Tonon et

al., 2011). However, the results revealed that MS/MD possessed both the lowest moisture content and the lowest hygroscopicity. The larger particle size of MS/MD compared to other powders may reduce the exposure area of the particles to atmospheric moisture, contributing to its lower hygroscopicity. In contrast, moisture absorption by GA/MD is attributed to the presence of hydrogen ( $H_2$ ) in water molecules and the hydroxyl groups present in GA and MD. In this study, the hygroscopicity values of microencapsulated gurun seed oil were lower than those reported in previous studies using GA as the wall material, such as Gagaita fruit extract (14.8–18.8%) (Daza et al., 2016), and rosemary essential oil (15.9–18.9%) (de Barros Fernandes et al., 2014). Similar findings were reported by Chew et al. (Chew et al., 2018), for microencapsulated refined kenaf seed oil (7.8–10.1%).

### 3.5. Wettability

Wettability refers to a powder's ability to absorb a liquid due to capillary forces, with shorter dissolution times indicating better physical properties and potential applications in the food industry (Chew et al., 2018). **Table 2** presents the wettability data for all freshly microencapsulated MLCTs rich SLs. The results indicated that MS/MD exhibited a wettability of 575 s, whereas GA/MD and MIX showed wettability times of 290 s and 744 s, respectively. Notably, the use of GA and MD in a 2:1 ratio reduced the wettability time compared to MS/MD and MIX formulations. This finding aligns with Dima et al.'s observation that decreasing particle size increases wettability time, consistent with the results of this study (Dima et al., 2016).

### 3.6. Solubility

Solubility marks the last stage of particle dissolution and holds significant importance in assessing food quality (de Barros Fernandes et al., 2014). Powders with poor solubility can lead to processing challenges and economic losses. The results indicated that all powders exhibited solubility, ranging from 86.27% to 92.84% (**Table 2**). MLCTs rich SLs are typically insoluble in water at room temperature. However, the wall materials utilized for encapsulating the MLCTs rich SLs contributed to enhancing their solubility.

Table 2. Encapsulation yield, M.E.E., moisture content, water activity, hygroscopicity, wettability and solubility.

Treatments	MS/MD	GA/MD	MIX
Encapsulation yield (%)	85.34±0.05 <sup>c</sup>	93.23±0.03 <sup>a</sup>	89.88±0.03 <sup>b</sup>
M.E.E (%)	90.34±0.04 <sup>c</sup>	93.74±0.03 <sup>a</sup>	91.65±0.05 <sup>b</sup>
Moisture content (%)	3.45±0.05 <sup>a</sup>	1.71±0.04 <sup>c</sup>	2.66±0.03 <sup>b</sup>
Water activity	0.31±0.01 <sup>a</sup>	0.17±0.01 <sup>c</sup>	0.24±0.02 <sup>b</sup>
Hygroscopicity (g/100g)	6.75±0.01 <sup>c</sup>	7.44±0.04 <sup>b</sup>	8.67±0.05 <sup>a</sup>

Wettability (s)	575.33±4.51 <sup>b</sup>	290.67±4.04 <sup>c</sup>	744±4 <sup>a</sup>
Solubility (%)	88.72±0.03 <sup>b</sup>	92.84±0.04 <sup>a</sup>	86.27±0.03 <sup>c</sup>

**Abbreviations:** MS/MD = modified starch/ maltodextrin; GA/MD = gum Arabic/ maltodextrin; MIX = mixed; M.E.E = microencapsulation efficiency. Data presented as means of triplicate ±SD. Data with the different superscript letters (within a column, a,b,c) are significantly different ( $p < 0.05$ ).

### 3.7. Bulk density (BD)

The bulk density of microencapsulated MLCTs rich SLs varied from 0.15 to 0.25 g.cm<sup>-3</sup> for MS/MD, GA/MD, and MIX formulations (Table 3). These results fell within the expected range for bulk density in microencapsulated powders, as reported in previous models (Carneiro et al., 2013). Notably, MS/MD exhibited the lowest bulk density among the GA/MD and MIX microencapsulated MLCTs rich SLs. This difference underscores the significant influence of the wall material on the bulk density of microencapsulated MLCTs rich SLs. The lower bulk density observed in MS/MD formulations may be attributed to the spongy nature of the microcapsule wall produced by MS/MD. This characteristic is likely influenced by the higher proportion of MS in the MS/MD model, which has a distinct impact on bulk density. Additionally, the larger particle size of MS/MD microencapsulated MLCTs rich SLs contributes to lower particle density, as density decreases with an increase in volume for a fixed mass product (Goyal et al., 2015). Our study observed a similar trend, where bulk density decreased with increasing particle size. Conversely, the higher solid content in GA/MD and MIX microencapsulated formulations would contribute to increased bulk density. When compared to microencapsulated flaxseed oil using MD mixed with whey protein concentrate (WPC) and MS, GA mixed with MD tended to produce denser particles (Carneiro et al., 2013).

### 3.8. Tapped density (TD) and particle density (PD)

Tapped density is a critical factor, affecting the packaging, transportation, and commercialization of powders. In the case of microencapsulated MLCTs rich SLs, the tapped density ranged from 0.33 to 0.43 g.cm<sup>-3</sup> for MS/MD, GA/MD, and MIX formulations (Table 3). In our study, GA/MD microencapsulated MLCTs rich SLs exhibited the highest tapped density, followed by the MIX microencapsulated formulation. The ratio of the wall material significantly influenced the tapped density, with the use of MS together with MD resulting in lower tapped density in MS/MD-microencapsulated MLCTs rich SLs. Powders generated through spray-drying typically exhibit high tapped density, which is advantageous for storing them in small containers conveniently. Moreover, higher bulk density indicates a lesser amount of air in the powders,

which can help prevent fat oxidation during storage (Carneiro et al., 2013).

The particle density of microencapsulated MLCTs rich SLs ranged from 0.81 to 1.25 g.cm<sup>-3</sup> in this study. MS/MD microencapsulated MLCTs rich SLs demonstrated significantly lower particle density ( $p < 0.05$ ) compared to GA/MD and MIX microencapsulated formulations. This observation can be attributed to MS/MD contributing to lower PD compared to GA. The particle density of GA/MD and MIX microcapsules was similar to that reported by Fernandes et al. (de Barros Fernandes et al., 2014), who used GA to microencapsulate rosemary essential oil (1.0-1.3 g mL<sup>-1</sup>).

### 3.9. Flowability, cohesiveness, and bulk porosity

The Carr's Index (CI) evaluates the free-flowing characteristic, while the Hausner ratio (HR) evaluates the cohesiveness of the powders. In this study, the results showed that the CI was in the range of 41.86-54.55, indicating awful flowability (Table 4). The HR was in the range of 1.72-2.20 for the developed microencapsulated MLCTs rich SLs. The higher HR indicates that the powders are more cohesive and have lower ability to flowability. GA/MD-microencapsulated MLCTs rich SLs displayed significantly lowest ( $p < 0.05$ ) CI and HR values among the MS/MD and MIX-microencapsulated MLCTs rich SLs. This showed that the GA could contribute better flowability than the MS. Anyway, there were previous studies reported awful flowability of the powders with high CI values (33.7-48.7) in flaxseed oil microcapsules (Carneiro et al., 2013), in sunflower oil microcapsules (Goyal et al., 2015), and fish oil microcapsules (Kagami et al., 2003).

Bulk porosity (BP) is an important property in food processing, especially in the reconstitution of dry powder. In this study, the results showed that the bulk porosity of MIX-microencapsulated MLCTs rich SLs was significantly different ( $p < 0.05$ ) than that of MS/MD and GA/MD-microencapsulated MLCTs rich SLs. MS and MD contributed to the lowest bulk porosity of MS/MD microencapsulated MLCTs rich SLs between the microcapsules produced. However, the bulk porosity values in this study were lower than the values (70.0-74.5%) reported by Jinapong et al. (Jinapong et al., 2008), in soy milk powders. The large contents of bulk porosity indicate the presence of a big number of wipers among the particles,

which holding O<sub>2</sub> that causes degradation reactions (Santhalakshmy et al., 2015).

Table 3. Bulk density, tapped density, particle density, Carr index (CI), Hausner ratio (HR), and flowability of the gurum seed oil microcapsule powders.

Treatments	MS/MD	GA/MD	MIX
Bulk density (g cm <sup>-3</sup> )	0.15±0.01 <sup>c</sup>	0.25±0.03 <sup>a</sup>	0.23±0.02 <sup>b</sup>
Tapped density (g cm <sup>-3</sup> )	0.33±0.04 <sup>c</sup>	0.43±0.03 <sup>a</sup>	0.41±0.01 <sup>b</sup>
Particle density (g cm <sup>-3</sup> )	0.81±0.02 <sup>c</sup>	1.25±0.03 <sup>a</sup>	1.02±0.01 <sup>b</sup>
Bulk porosity (%)	48.94±0.04 <sup>c</sup>	65.03±0.02 <sup>b</sup>	66.1±0.03 <sup>a</sup>
Carr Index (%)	54.55±0.05 <sup>a</sup>	41.86±0.03 <sup>c</sup>	43.9±0.03 <sup>b</sup>
Hausner Ratio (HR)	2.20±0.05 <sup>a</sup>	1.72±0.04 <sup>c</sup>	1.78±0.03 <sup>b</sup>
Flowability	Awful	Awful	Awful

**Abbreviations:** MS/MD = modified starch/ maltodextrin; GA/MD = gum Arabic/ maltodextrin; MIX = mixed; M.E.E = microencapsulation efficiency. Data presented as means of triplicate ±SD. Data with the different superscript letters (within a column, a,b,c) are significantly different (p < 0.05).

Table 4. Flowability and cohesiveness from the Carr's index and Hausner ratio (HR).

Flowability	Carr index (%)	Hausner ratio (HR)
Excellent	0-10	1.00–1.11
Good	11–15	1.12–1.18
Fair	16-20	1.19–1.25
Passable	21-25	1.26–1.34
Poor	26–31	1.35–1.45
Very poor	32–37	1.46–1.59
Awful	>38	>1.60

### 3.10. Color

The color parameters, which include luminosity (L\* representing the degree of lightness on a scale from 0 to 100 where 0 is black and 100 is white), a\* (representing the degree of redness (+) to greenness (-)), and b\* (representing the degree of yellowness (+) to blueness (-)), are presented in **Table 5** (Korma et al., 2019).

Table 5. Color parameters of the MLCTs rich SLs microencapsulated powder.

Parameters	L*	a*	b*
MS/MD	94.89±0.04 <sup>b</sup>	-0.78±0.02 <sup>a</sup>	9.02±0.04 <sup>a</sup>
GA/MD	95.60±0.02 <sup>a</sup>	-0.52±0.03 <sup>c</sup>	7.25±0.03 <sup>c</sup>
MIX	94.75±0.05 <sup>c</sup>	-0.70±0.04 <sup>b</sup>	8.16±0.03 <sup>b</sup>

L\* (luminosity degree), a\* (degree of redness to greenness), b\* (degree of yellowness to blueness). The results are expressed as the mean value ± standard deviation (n=3). Different letters in the same column indicate significant differences (p ≤ 0.05) between the data.

As can be seen in **Table 5**, there were no significant differences (p ≤ 0.05) observed among the mean values of lightness (L\*) for the microcapsule powder formulations investigated in this study. The lightness mean

values (L\*) ranged from 94.75 to 95.60, suggesting that all samples tended to be of white color.

The mean values of a\* ranged from -0.52 to -0.78, indicating a tendency towards green color for all samples.

Notably, the GA/MD formulation exhibited a significantly lower ( $p \leq 0.05$ ) mean value of  $a^*$  compared to other formulations.

Regarding the mean values of  $b^*$ , they ranged from 7.25 to 9.02, suggesting a tendency towards yellow color for all samples. The GA/MD formulation showed a significantly lower ( $p \leq 0.05$ ) mean value of  $b^*$  compared to other formulations. This difference could be attributed to its high whey protein content.

### 3.11. Crystallinity (X-ray diffraction)

Determining whether encapsulated substances possess crystalline or amorphous structures is crucial for understanding their stability, often analyzed through XRD. The XRD patterns of microencapsulated MLCT-rich SLs powders are depicted in **Fig 1**. The relative crystallinity

observed in MS/MD, GA/MD, and MIX microencapsulated MLCT-rich SLs ranged from 30.28% to 32.50%. Among these, GA/MD-microencapsulated MLCT-rich SLs exhibited the highest relative crystallinity, followed by MS/MD microencapsulated MLCT-rich SLs. The results suggest that the MIX model, incorporating MS, GA, and MD in a 1:1:1 ratio, exhibits a slight inclination towards crystallization. Additionally, the GA/MD model may offer enhanced storage stability due to its higher relative crystallinity compared to other models. Generally, amorphous samples tend to be hygroscopic, absorbing more water during storage. This propensity for water absorption can lead to weight gain, nutrient degradation, breakdown of microstructure, and increased microbiological instability, ultimately compromising sample quality during storage (Borrmann et al., 2013).

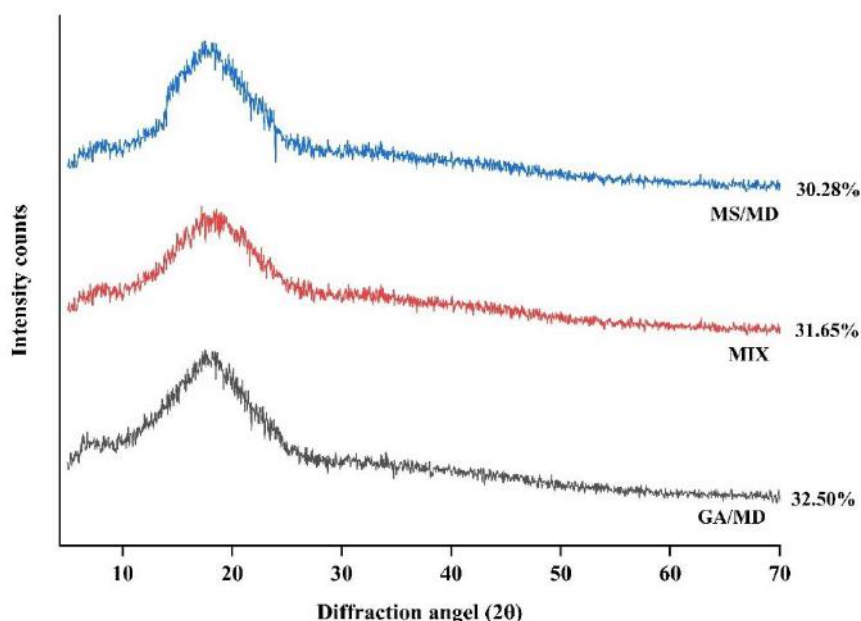


Fig. 1. Relative crystallinity by X-ray diffraction patterns of MLCTs rich SLs rich microcapsule powders, MS/MD: modified starch/maltodextrin; GA/MD: gum Arabic/ maltodextrin; MIX: Mixed

### 3.12. Fourier transform infrared spectroscopy (FTIR)

FTIR analysis was used to investigate the characteristics of MS/MD, GA/MD, and MIX microcapsules containing MLCTs rich SLs. The spectra displayed in **Fig. 2** included fish oil, interesterified product (MLCTs rich SLs), MD, GA, MS, and the microcapsules (MS/MD, GA/MD, and MIX). Fish oil and MLCT-rich SLs exhibited absorbance at 720 and 2853  $\text{cm}^{-1}$ , indicating the presence of DHA in unencapsulated fish oil and MLCTs rich SLs. The spectral range spanning from 2923 to 2852  $\text{cm}^{-1}$  indicated the presence of PUFA, while wavelengths

falling between 1743 and 1746  $\text{cm}^{-1}$  suggested the presence of ester carbonyl (Bekhit et al., 2014; Sinclair et al., 1952). Additionally, the regions around 720  $\text{cm}^{-1}$  indicated the presence of FAs with cis double bonds in unencapsulated fish oil and MLCTs rich SLs (Karthik & Anandharamakrishnan, 2013). Additionally, fish oil showed a flat O-H stretching at 3425  $\text{cm}^{-1}$ , whereas MLCTs rich SLs showed a slight bend at the same wavelength. The band observed at 1158  $\text{cm}^{-1}$  in both fish oil and MLCTs rich SLs corresponded to the C-O-C stretching (Bhandari & Howes, 1999; de Barros Fernandes et al., 2016). The MD spectrum showed absorption bands at 3290  $\text{cm}^{-1}$  (O-H

stretching),  $2928\text{ cm}^{-1}$  (C-H stretching from the carboxylic group),  $1644\text{ cm}^{-1}$  (C=O stretching),  $1355\text{ cm}^{-1}$  (O-H bending), and  $1155, 1079, 1007\text{ cm}^{-1}$  (C-O stretching and C-O-H bending). These findings are similar with those reported by Chew et al. (Chew et al., 2018). Similarly, GA displayed absorption bands at  $3278\text{ cm}^{-1}$  (O-H stretching),  $2918\text{ cm}^{-1}$  (C-H stretching from the carboxylic group),  $1604\text{ cm}^{-1}$  (C=O stretching or N-H bending),  $1410\text{ cm}^{-1}$  (CH<sub>3</sub> bending and C-H bending), and  $1020\text{ cm}^{-1}$  (C-O stretching), similar results were reported by Chew et al. (Chew et al., 2018). The FTIR spectra revealed absorption bands of MS at specific wavenumbers:  $3275\text{ cm}^{-1}$  (O-H stretching),  $2938\text{ cm}^{-1}$  (C-H stretching from the carboxylic group),  $1641\text{ cm}^{-1}$  (C=O stretching),  $1335\text{ cm}^{-1}$  (CH<sub>3</sub> bending), and  $1145\text{ cm}^{-1}$ ,  $1074\text{ cm}^{-1}$ , and  $993\text{ cm}^{-1}$  (C-O stretching and C-O-H bending). These findings were similar with previous studies (Chew et al., 2018; Hosseinnia et al., 2017), indicating consistency in the observed spectral characteristics of MS.

The presence of bands at  $1743, 1158, 2853,$  and  $2922\text{ cm}^{-1}$  in fish oil and MLCTs rich SLs was notably reduced in MS/MD, GA/MD and MIX-microencapsulated samples, suggesting successful encapsulation of the oil into the microcapsules (Hu et al., 2016). In this study, all microcapsule powders exhibited prominent hydroxyl peaks (O-H stretching) at  $3288\text{ cm}^{-1}$ , as well as carboxylic group peaks (C-H stretching) at  $2925\text{ cm}^{-1}$ . The occurrence of C=O stretching and C-O-H bending at  $1155, 1079,$  and  $1007\text{ cm}^{-1}$  was observed in all formulations (Chew et al., 2018; Hosseinnia et al., 2017; Mahdi et al., 2020). MS/MD and MIX-based microcapsules exhibited profiles closely resembling gum Arabic, with gum Arabic being the predominant component in these formulations. The absence of amide groups were observed in all the formulations it may be due to the absence of whey protein (Mahdi et al., 2020).

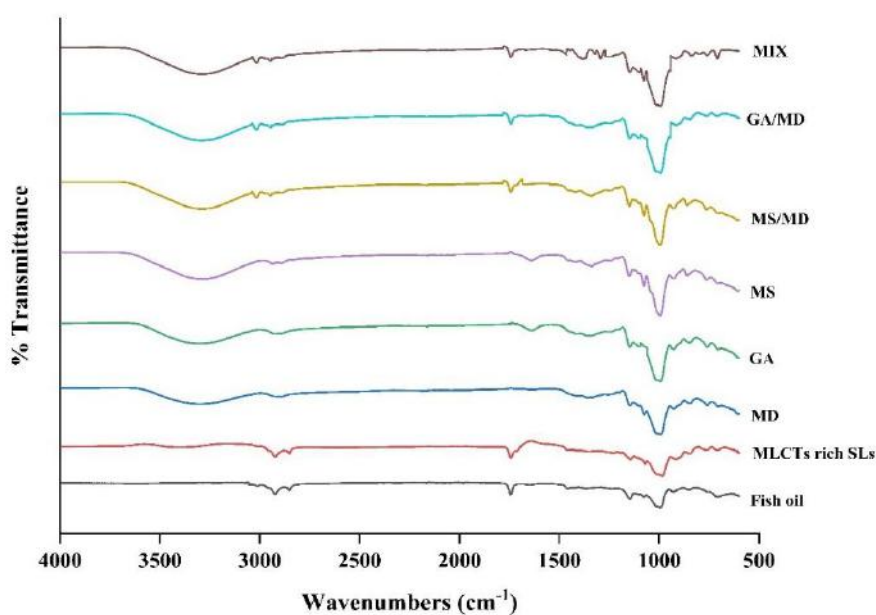


Fig. 2. FTIR spectra of raw materials (gum Arabic (GA), maltodextrin (MD), modified starch (MS), the microcapsules (MS/MD, GA/MD, MIX) MLCTs rich SLs and fish oil..

### 3.13. Scanning electron microscope (SEM)

SEM analysis was conducted on the microencapsulated MLCTs rich SLs powders, as depicted in Fig. 3. The purpose was to examine for any potential defects like fractures or cracks that could compromise the coherence of the encapsulated material, certain that such defects could lead to degradation and oxidation (Guadarrama-Lezama et al., 2012). The SEM micrographs revealed spherical and semi-spherical shapes of the microcapsules, although spray-dried particles typically exhibit a spherical shape with a

mean size ranging from 10 to 100 nm (Fang & Bhandari, 2010). Variations in morphologies and irregular surfaces were likely influenced by differences in feeding ratio, droplet size, and drying temperature during the process. Shrinkage followed by potential expansion could change particle size and lead to broken shells. Moreover, surface irregularities on the microcapsules could enhance dispersibility and rehydration of the powders (Guadarrama-Lezama et al., 2012). MLCTs rich SLs microencapsulated with MD/MS, GA/MD, and MIX did not exhibit any fissures or cracking. This suggests that microencapsulation

of MLCTs rich SLs with these wall materials could yield microencapsulated products with improved retention and stability. Hollow spheres, characteristic of spray-dried powders, were observed in MIX microcapsules (Hu et al., 2016). These findings are similar with previous studies using GA as carriers, they also observed spherical shapes

and irregularities due to shrinkage in various SEM studies (Chew et al., 2018; Daza et al., 2016; de Barros Fernandes et al., 2016). Similar morphological characteristics in all microcapsules indicate a uniform drying process, while surface shrinkage may result from the drying process.

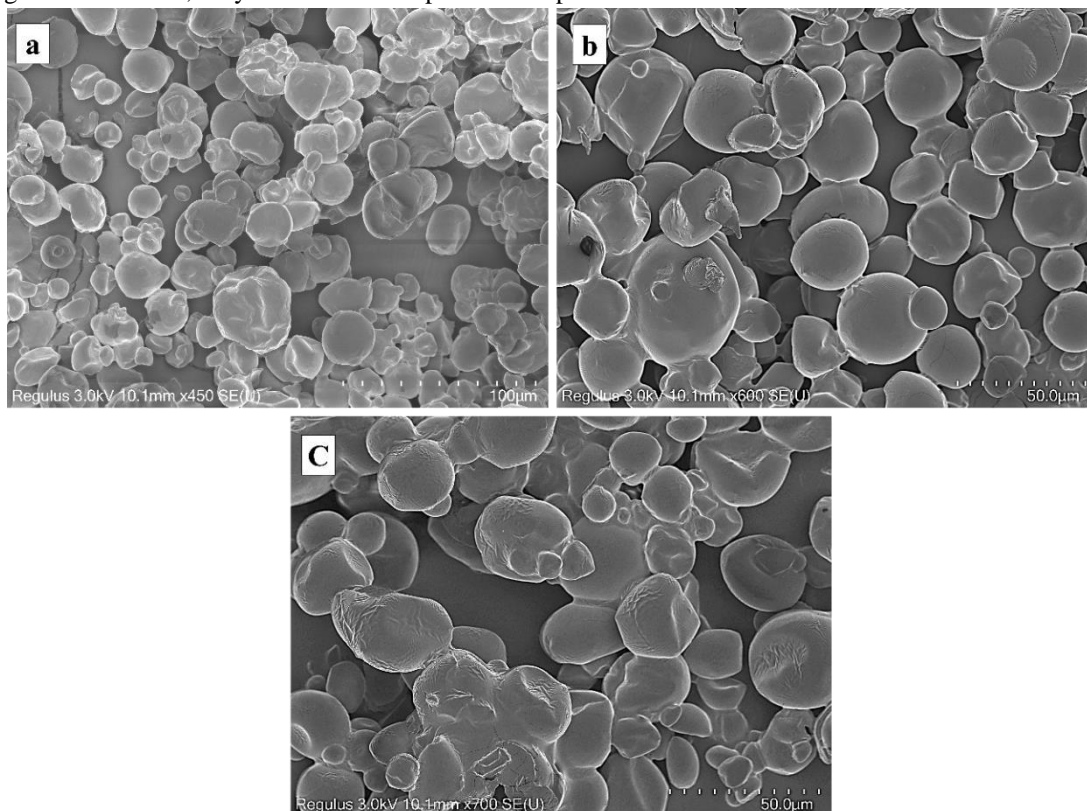


Fig. 3. SEM of MLCTs rich SLs microcapsule powders, (a) MS/MD, (b) GA/MD, (c) MIX: Mixed.

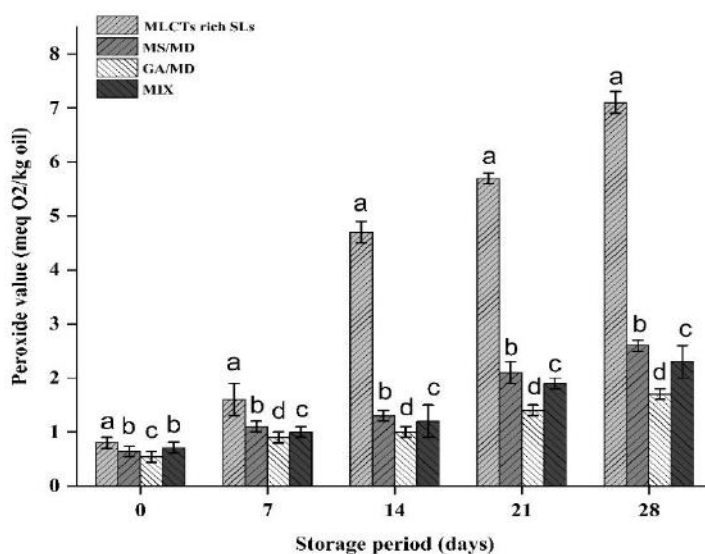


Fig 4. Peroxide values of microencapsulated MLCTs rich SLs and non-encapsulated SLs upon accelerated storage at 60 °C. MS/MD, GA/MD and MIX: Mixed

### 3.14. Oxidative stability under accelerated storage

The primary oxidative by-product of fat and oil is hydroperoxide, typically measured through peroxide value (PV) determination (Korma et al., 2019). The progression of peroxide values in both non-encapsulated MLCTs rich SLs and microencapsulated samples over seven-day intervals of storage at 60°C is illustrated in **Fig 4**. At the beginning of storage, MLCTs rich SLs exhibited a PV of 0.81 meq O<sub>2</sub>/kg, which did not significantly differ ( $p > 0.05$ ) from the PVs of microencapsulated oils, measuring 0.64, 0.55, and 0.72 meq O<sub>2</sub>/kg oil for MS/MD, GA/MD, and MIX microcapsules, respectively. These findings indicate that the applied spray drying method did not adversely affect the peroxidation of MLCTs rich SLs. However, the PV increased more rapidly in raw MLCTs rich SLs than in encapsulated samples over 14 days of storage. While slight increases in PV were observed in MS/MD and MIX microcapsules after 14 days, no significant variation was noted in GA/MD microcapsules. By day 28 of storage at 60°C, the PV of MLCTs rich SLs reached 7.21 meq O<sub>2</sub>/kg oil, whereas those of MS/MD and MIX microcapsules were 2.62 and 2.33 meq O<sub>2</sub>/kg oil, respectively. These findings reveal that GA/MD microcapsules exhibited superior oxidative stability compared to MS/MD and MIX microcapsules. These results are consistent with those reported by Premi et al. (Premi & Sharma, 2017), who observed high oil stability of encapsulated drumstick oil powder (EDOP) with MD and GA. MLCTs rich SLs, being rich in unsaturated fatty acids (UFA), is susceptible to oxidative degradation, leading to the formation of free radicals (hydroperoxides) during processing and storage. This susceptibility may account for the increasing peroxide value of non-encapsulated MLCTs rich SLs during storage. Overall, the microencapsulation of MLCTs rich SLs improved its oxidative stability, with the greatest enhancement observed when carbohydrate-based materials were used.

## IV. CONCLUSIONS

The MLCTs rich SLs were microencapsulated and spray-dried into a powder. Three treatments including MS/MD (2:1), GA/MD (2:1), and MIX (1:1:1) were used as wall material combinations, and all of them exhibited well visible microcapsules. The microcapsules produced using GA/MD were selected as the optimal encapsulation process due to their dominance across various properties. They exhibited the highest encapsulation yield and efficiency. Additionally, GA/MD microcapsules demonstrated the highest bulk, tapped, and particle density, indicating excellent storage stability. Conversely, they had the lowest

porosity and required a shorter time for wettability, suggesting a strong ability to reconstitute the powders. Moreover, X-ray diffraction analysis revealed that GA/MD microcapsules exhibited the highest relative crystallinity, indicating higher storage stability compared to other formulations. Overall, GA/MD microencapsulation offers an efficient approach for developing MLCTs rich SLs microcapsules with enhanced stability, making them potentially valuable as functional food and pharmaceutical ingredients.

## FUNDING

This work was supported by the National Natural Science Foundation of China (31601433)

## REFERENCES

- [1] Ackman, R. G., & Burgher, R. (1963). Component fatty acids of the milk of the grey (Atlantic) seal. *Canadian Journal of Biochemistry and Physiology*, 41(12), 2501-2505.
- [2] AL-Ansi, W., Mahdi, A. A., Al-Maqtari, Q. A., Fan, M., Wang, L., Li, Y., Qian, H., & Zhang, H. (2019). Evaluating the role of microwave-baking and fennel (*Foeniculum vulgare L.*)/nigella (*Nigella sativa L.*) on acrylamide growth and antioxidants potential in biscuits. *Journal of Food Measurement and Characterization*, 13, 2426-2437.
- [3] Bae, E., & Lee, S. J. (2008). Microencapsulation of avocado oil by spray drying using whey protein and maltodextrin. *Journal of Microencapsulation*, 25(8), 549-560.
- [4] Bakry, A. M., Abbas, S., Ali, B., Majeed, H., Abouelwafa, M. Y., Mousa, A., & Liang, L. (2016). Microencapsulation of oils: A comprehensive review of benefits, techniques, and applications. *Comprehensive reviews in food science and food safety*, 15(1), 143-182.
- [5] Bekhit, M. Y., Grung, B., & Mjøs, S. A. (2014). Determination of omega-3 fatty acids in fish oil supplements using vibrational spectroscopy and chemometric methods. *Applied spectroscopy*, 68(10), 1190-1200.
- [6] Bhandari, B., & Howes, T. (1999). Implication of glass transition for the drying and stability of dried foods. *Journal of Food Engineering*, 40(1-2), 71-79.
- [7] Bligh, E. G., & Dyer, W. J. (1959). A rapid method of total lipid extraction and purification. *Canadian Journal of Biochemistry and Physiology*, 37(8), 911-917.
- [8] Borrmann, D., Pierucci, A. P. T. R., Leite, S. G. F., & da Rocha Leão, M. H. M. (2013). Microencapsulation of passion fruit (*Passiflora*) juice with n-octenylsuccinate-derivatised starch using spray-drying. *Food and Bioproducts Processing*, 91(1), 23-27.
- [9] Cai, Y.-Z., & Corke, H. (2000). Production and properties of spray-dried *Amaranthus betacyanin* pigments. *Journal of Food Science*, 65(7), 1248-1252.
- [10] Calder, P. C. (2020). Eicosapentaenoic and docosahexaenoic acid derived specialised pro-resolving mediators: Concentrations in humans and the effects of age, sex, disease

- and increased omega-3 fatty acid intake. *Biochimie*, 178, 105-123.
- [11] Carneiro, H. C., Tonon, R. V., Grosso, C. R., & Hubinger, M. D. (2013). Encapsulation efficiency and oxidative stability of flaxseed oil microencapsulated by spray drying using different combinations of wall materials. *Journal of Food Engineering*, 115(4), 443-451.
- [12] Chew, S. C., Tan, C. P., & Nyam, K. L. (2018). Microencapsulation of refined kenaf (*Hibiscus cannabinus* L.) seed oil by spray drying using  $\beta$ -cyclodextrin/gum arabic/sodium caseinate. *Journal of Food Engineering*, 237, 78-85.
- [13] Daza, L. D., Fujita, A., Fávoro-Trindade, C. S., Rodrigues-Ract, J. N., Granato, D., & Genovese, M. I. (2016). Effect of spray drying conditions on the physical properties of Cagaita (*Eugenia dysenterica* DC.) fruit extracts. *Food and Bioproducts Processing*, 97, 20-29.
- [14] de Barros Fernandes, R. V., Borges, S. V., & Botrel, D. A. (2014). Gum arabic/starch/maltodextrin/inulin as wall materials on the microencapsulation of rosemary essential oil. *Carbohydrate polymers*, 101, 524-532.
- [15] de Barros Fernandes, R. V., Borges, S. V., Silva, E. K., da Silva, Y. F., de Souza, H. J. B., do Carmo, E. L., de Oliveira, C. R., Yoshida, M. I., & Botrel, D. A. (2016). Study of ultrasound-assisted emulsions on microencapsulation of ginger essential oil by spray drying. *Industrial crops and products*, 94, 413-423.
- [16] de Souza, V. B., Thomazini, M., Barrientos, M. A. E., Nalin, C. M., Ferro-Furtado, R., Genovese, M. I., & Favaro-Trindade, C. S. (2018). Functional properties and encapsulation of a proanthocyanidin-rich cinnamon extract (*Cinnamomum zeylanicum*) by complex coacervation using gelatin and different polysaccharides. *Food Hydrocolloids*, 77, 297-306.
- [17] Dima, C., Pătrașcu, L., Cantaragiu, A., Alexe, P., & Dima, Ș. (2016). The kinetics of the swelling process and the release mechanisms of *Coriandrum sativum* L. essential oil from chitosan/alginate/inulin microcapsules. *Food Chemistry*, 195, 39-48.
- [18] Drusch, S., & Schwarz, K. (2006). Microencapsulation properties of two different types of n-octenylsuccinate-derivatised starch. *European Food Research and Technology*, 222, 155-164.
- [19] Du, J., Ge, Z.-Z., Xu, Z., Zou, B., Zhang, Y., & Li, C.-M. (2014). Comparison of the efficiency of five different drying carriers on the spray drying of persimmon pulp powders. *Drying technology*, 32(10), 1157-1166.
- [20] Fang, Z., & Bhandari, B. (2010). Encapsulation of polyphenols—a review. *Trends in food science & technology*, 21(10), 510-523.
- [21] Firestone, D. (1989). Official methods and recommended practices of the American Oil Chemists' Society. (*No Title*).
- [22] Goyal, A., Sharma, V., Sihag, M. K., Tomar, S., Arora, S., Sabikhi, L., & Singh, A. (2015). Development and physico-chemical characterization of microencapsulated flaxseed oil powder: A functional ingredient for omega-3 fortification. *Powder Technology*, 286, 527-537.
- [23] Guadarrama-Lezama, A. Y., Dorantes-Alvarez, L., Jaramillo-Flores, M. E., Pérez-Alonso, C., Niranjana, K., Gutiérrez-López, G. F., & Alamilla-Beltrán, L. (2012). Preparation and characterization of non-aqueous extracts from chilli (*Capsicum annum* L.) and their microencapsulates obtained by spray-drying. *Journal of Food Engineering*, 112(1-2), 29-37.
- [24] Hosseinnia, M., Khaledabad, M. A., & Almasi, H. (2017). Optimization of *Ziziphora clinopodioides* essential oil microencapsulation by whey protein isolate and pectin: A comparative study. *International Journal of Biological Macromolecules*, 101, 958-966.
- [25] Hu, L., Zhang, J., Hu, Q., Gao, N., Wang, S., Sun, Y., & Yang, X. (2016). Microencapsulation of *brucea javanica* oil: Characterization, stability and optimization of spray drying conditions. *Journal of Drug Delivery Science and Technology*, 36, 46-54.
- [26] Hu, Y., Li, Y., Zhang, W., Kou, G., & Zhou, Z. (2018). Physical stability and antioxidant activity of citrus flavonoids in arabic gum-stabilized microcapsules: Modulation of whey protein concentrate. *Food Hydrocolloids*, 77, 588-597.
- [27] Jiang, H., Wang, L., Wang, D., Yan, N., Li, C., Wu, M., Wang, F., Mi, B., Chen, F., & Jia, W. (2022). Omega-3 polyunsaturated fatty acid biomarkers and risk of type 2 diabetes, cardiovascular disease, cancer, and mortality. *Clinical Nutrition*, 41(8), 1798-1807.
- [28] Jinapong, N., Suphantharika, M., & Jamnong, P. (2008). Production of instant soymilk powders by ultrafiltration, spray drying and fluidized bed agglomeration. *Journal of Food Engineering*, 84(2), 194-205.
- [29] Kagami, Y., Sugimura, S., Fujishima, N., Matsuda, K., Kometani, T., & Matsumura, Y. (2003). Oxidative stability, structure, and physical characteristics of microcapsules formed by spray drying of fish oil with protein and dextrin wall materials. *Journal of Food Science*, 68(7), 2248-2255.
- [30] Kang, Y.-R., Lee, Y.-K., Kim, Y. J., & Chang, Y. H. (2019). Characterization and storage stability of chlorophylls microencapsulated in different combination of gum Arabic and maltodextrin. *Food Chemistry*, 272, 337-346.
- [31] Karaca, A. C., Nickerson, M., & Low, N. H. (2013). Microcapsule production employing chickpea or lentil protein isolates and maltodextrin: Physicochemical properties and oxidative protection of encapsulated flaxseed oil. *Food Chemistry*, 139(1-4), 448-457.
- [32] Karthik, P., & Anandharamakrishnan, C. (2013). Microencapsulation of docosahexaenoic acid by spray-freeze-drying method and comparison of its stability with spray-drying and freeze-drying methods. *Food and Bioprocess Technology*, 6, 2780-2790.
- [33] Khan, I., Hussain, M., Jiang, B., Zheng, L., Pan, Y., Hu, J., Khan, A., Ashraf, A., & Zou, X. (2023). Omega-3 long-chain polyunsaturated fatty acids: Metabolism and health implications. *Progress in Lipid Research*, 101255.
- [34] Korma, S. A., Wei, W., Ali, A. H., Abed, S. M., Zheng, L., Jin, Q., & Wang, X. (2019). Spray-dried novel structured lipids enriched with medium-and long-chain triacylglycerols encapsulated with different wall materials: Characterization and stability. *Food Research International*, 116, 538-547.

- [35] Korma, S. A., Zou, X., Ali, A. H., Abed, S. M., Jin, Q., & Wang, X. (2018). Preparation of structured lipids enriched with medium-and long-chain triacylglycerols by enzymatic interesterification for infant formula. *Food and Bioprocess Technology*, 107, 121-130.
- [36] Lee, Y.-Y., Tang, T.-K., Tan, C.-P., Alitheen, N. B. M., Phuah, E.-T., Karim, N. A. A., & Lai, O.-M. (2015). Entrapment of palm-based medium-and long-chain triacylglycerol via maillard reaction products. *Food and Bioprocess Technology*, 8, 1571-1582.
- [37] Li, Z., Wang, L., Chen, Z., Yu, Q., & Feng, W. (2018). Impact of binding interaction characteristics on physicochemical, structural, and rheological properties of waxy rice flour. *Food Chemistry*, 266, 551-556.
- [38] Lu, J., Jin, Q., Wang, X., & Wang, X. (2017). Preparation of medium and long chain triacylglycerols by lipase-catalyzed interesterification in a solvent-free system. *Process Biochemistry*, 54, 89-95.
- [39] Mahdi, A. A., Mohammed, J. K., Al-Ansi, W., Ghaleb, A. D., Al-Maqtari, Q. A., Ma, M., Ahmed, M. I., & Wang, H. (2020). Microencapsulation of fingered citron extract with gum arabic, modified starch, whey protein, and maltodextrin using spray drying. *International Journal of Biological Macromolecules*, 152, 1125-1134.
- [40] Ng, S.-K., Jessie, L.-Y. L., Tan, C.-P., Long, K., & Nyam, K.-L. (2013). Effect of accelerated storage on microencapsulated kenaf seed oil. *Journal of the American Oil Chemists' Society*, 90, 1023-1029.
- [41] Premi, M., & Sharma, H. (2017). Effect of different combinations of maltodextrin, gum arabic and whey protein concentrate on the encapsulation behavior and oxidative stability of spray dried drumstick (*Moringa oleifera*) oil. *International Journal of Biological Macromolecules*, 105, 1232-1240.
- [42] Saifullah, M., Yusof, Y., Chin, N., & Aziz, M. (2016). Physicochemical and flow properties of fruit powder and their effect on the dissolution of fast dissolving fruit powder tablets. *Powder Technology*, 301, 396-404.
- [43] Santhalakshmy, S., Bosco, S. J. D., Francis, S., & Sabeena, M. (2015). Effect of inlet temperature on physicochemical properties of spray-dried jamun fruit juice powder. *Powder Technology*, 274, 37-43.
- [44] Sinclair, R., McKay, A., Myers, G., & Jones, R. N. (1952). The infrared absorption spectra of unsaturated fatty acids and esters1. *Journal of the American Chemical Society*, 74(10), 2578-2585.
- [45] Tonon, R. V., Grosso, C. R., & Hubinger, M. D. (2011). Influence of emulsion composition and inlet air temperature on the microencapsulation of flaxseed oil by spray drying. *Food Research International*, 44(1), 282-289.